

STRUCTURE-PRESERVING MODEL REDUCTION ON MANIFOLDS OF PORT-HAMILTONIAN SYSTEMS

Silke Glas *

Hongliang Mu *

ABSTRACT

This paper considers structure-preserving model order reduction (MOR) techniques for port-Hamiltonian (pH) systems, which are typically derived from energy-based modelling. To keep favorable properties of pH systems such as stability and passivity in a reduced order model (ROM), we use structure-preserving methods in the reduction process. There exists an extensive literature on structure-preserving MOR methods of pH systems, however, to the best of our knowledge, there does not exist an intrusive structure-preserving MOR method for nonlinear pH systems on the base of general nonlinear approximation maps. To close this gap, we propose a MOR method for pH systems based on the idea of the generalized manifold Galerkin (GMG) reduction. The resulting MOR method can be applied to both linear and nonlinear pH systems resulting in ROMs, which are again of pH form. For the numerical examples, we employ a linear and a nonlinear mass-spring-damper system and the results show that the proposed MOR methods have lower relative reduction error compared to existing methods.

Keywords structure-preserving model reduction, port-Hamiltonian systems, generalized manifold Galerkin reduction, quadratically embedded manifolds

1 Introduction

Port-Hamiltonian (pH) systems are often derived via energy-based modelling, which is e.g., used for multi-physics systems, e.g., electrical circuits [9], mechanical systems [8], and fluid dynamics [5]. By using this type of modelling, a (big) overall system can be decomposed into subsystems, which are interconnected through their ports. An important property of these pH systems is that they satisfy an energy/power balance equation, i.e., the change in the Hamiltonian with respect to time equals the supplied energy minus the dissipated energy, which can be used to derive properties like stability and passivity. However, for a given high-dimensional pH system, its simulation can be computationally expensive. To overcome this bottleneck, model (order) reduction (MOR) techniques, which approximate the full-order model (FOM) by a reduced-order model (ROM), have been proposed. Some well-known MOR methods are, e.g., the proper orthogonal decomposition (POD) [29], the iterative rational Krylov algorithm (IRKA) [2], and the balanced truncation [19]. Unfortunately, the aforementioned MOR methods do not guarantee preservation of the pH structure in the ROM. However, in the last years multiple structure-preserving pH methods have been developed. In the following, we provide an overview of such methods and subsequently introduce our new method.

We first review MOR methods for linear pH systems. Moment matching-based MOR methods were introduced in [13, 31]. Based on this framework, pH-IRKA was proposed in [12]. The authors of [26] developed a Riemannian optimal MOR approach based on a trust region method. Furthermore, non-intrusive structure-preserving MOR methods, including pH-dynamic mode decomposition (pH DMD) [20], pH identification network (pHIN) [25], data-driven pH-operator inference (pH-Oplnf) [10], and structured optimization-based model order reduction (SOBMOR) [28], have been developed recently. For pH systems with nonlinear Hamiltonians, multiple MOR approaches have been introduced, where we provide an overview in the following. In [14], a moment matching-based MOR method for nonlinear pH systems was developed. A structure-preserving balanced truncation MOR method based on generalized Gramians was proposed in [16]. Moreover, a POD-based structure-preserving MOR technique was developed by considering a POD basis of the gradient of the Hamiltonian $\nabla_x \mathcal{H}(x)$ [6]. For pH systems with nonlinear Hamiltonian, it is important to note that the evaluation of the ROM still depends on the FOM dimension, even, if a

*Department of Applied Mathematics University of Twente Enschede, The Netherlands (s.m.glas@utwente.nl, h.l.mu@utwente.nl)

linear reduction technique is utilized. Therefore, structure-preserving discrete empirical interpolation methods (DEIM), which have been proposed in [6, 22], are typically applied to reduce computational complexity. When the FOM is an advection-dominated problem, its approximation quality using linear MOR methods might suffer from slowly decaying Kolmogorov n -widths, see e.g., [11, 21]. To overcome this limitation, nonlinear MOR methods can be used. For pH systems, the work of [27] recently introduced a nonlinear MOR method based on a special structure of the nonlinear embedding map.

In this work, we propose a novel structure-preserving MOR method of pH systems by using the generalized manifold Galerkin (GMG) reduction [4], and we analyze the existence of the GMG reduction map. In the following, we list some benefits of using the GMG reduction for pH systems: (i) the GMG reduction can be applied to nonlinear pH systems and can be used with a general nonlinear embedding map, extending the methods known in the literature. (ii) the resulting ROMs are again pH systems and (iii) our numerical results on a linear and nonlinear mass-spring-damper system show better accuracy compared to existing methods for using linear and quadratic embeddings.

The outline of this paper is as follows: in Section 2, we introduce pH systems, the GMG reduction and structure-preserving DEIM of pH systems. We propose the general novel MOR technique that preserves the pH structure and is based on the GMG reduction in Section 3. In Section 4, we detail how the ROM is derived for a linear and a quadratic embedding functions and the numerical results on a linear and nonlinear mass-spring-damper system are discussed in Section 5. We conclude and discuss possible extensions of this work in Section 6.

2 Preliminaries

In this section, we introduce the necessary background information needed for the readability of the paper. We start in Section 2.1 with a definition of pH systems and their properties. Afterwards, we recall the generalized manifold Galerkin (GMG) reduction in Section 2.2 and subsequently introduce the well-known DEIM method for nonlinear pH systems in Section 2.3, as it is needed in our numerical experiments.

2.1 Introduction to port-Hamiltonian systems

In this paper, we consider N -dimensional *input-state-output port-Hamiltonian (pH) systems* of the form²

$$\Sigma(\mathbf{J}, \mathbf{R}, \mathcal{H}, \mathbf{B}, \mathbf{u}, \mathbf{y}, \mathbf{x}_0) := \begin{cases} \frac{d}{dt} \mathbf{x}(t) &= (\mathbf{J} - \mathbf{R}) \nabla_{\mathbf{x}} \mathcal{H}(\mathbf{x}(t)) + \mathbf{B} \mathbf{u}(t), \\ \mathbf{y}(t) &= \mathbf{B}^\top \nabla_{\mathbf{x}} \mathcal{H}(\mathbf{x}(t)), \quad \mathbf{x}(t_0) = \mathbf{x}_0, \end{cases} \quad (1)$$

with state $\mathbf{x}(t) \in \mathbb{R}^N$, input $\mathbf{u}(t) \in \mathbb{R}^m$, output $\mathbf{y}(t) \in \mathbb{R}^m$ on time interval $\mathcal{I} := (t_0, t_{\text{end}}]$ and initial condition $\mathbf{x}_0 \in \mathbb{R}^N$. This pH system exchanges energy to its environment via ports, and $\mathbf{B} \in \mathbb{R}^{N \times m}$, also called port-matrix, describes this exchange. The function $\mathcal{H} \in \mathcal{C}^1(\mathbb{R}^N, \mathbb{R})$, called the *Hamiltonian*, represents the internal energy of the system and we assume, that has a strictly lower bound, i.e.,

$$\exists \mathbf{x}_e \in \mathbb{R}^N, \quad \mathcal{H}(\mathbf{x}) \geq \mathcal{H}(\mathbf{x}_e), \text{ for all } \mathbf{x} \neq \mathbf{x}_e.$$

Further, we have the matrices with respect to $\mathbf{J}, \mathbf{R} \in \mathbb{R}^{N \times N}$ related to the interconnection and dissipation of the system, which satisfy

$$\mathbf{J} = -\mathbf{J}^\top \in \mathbb{R}^{N \times N}, \quad 0 \leq \mathbf{R} = \mathbf{R}^\top \in \mathbb{R}^{N \times N}, \quad \det(\mathbf{J} - \mathbf{R}) \neq 0.$$

The latter condition, i.e., $\det(\mathbf{J} - \mathbf{R}) \neq 0$, is not included in the general definition of pH systems, but introduced by us for the remainder of this paper.

One important property of pH systems $\Sigma(\mathbf{J}, \mathbf{R}, \mathcal{H}, \mathbf{B}, \mathbf{u}, \mathbf{y}, \mathbf{x}_0)$ is, that they satisfy a power balance equation, i.e.,

$$\mathbf{y}(t)^\top \mathbf{u}(t) = \frac{d}{dt} \mathbf{x}(t)^\top \nabla_{\mathbf{x}} \mathcal{H} + (\mathbf{R} \nabla_{\mathbf{x}} \mathcal{H}(\mathbf{x}(t)))^\top \nabla_{\mathbf{x}} \mathcal{H}(\mathbf{x}(t)). \quad (2)$$

The equation above shows that the power supplied from the external ports is equal to the sum of the change of the Hamiltonian in the system and the dissipation of power [23]. Here, we denote $\mathbf{y}(t)^\top \mathbf{u}(t)$ and $(\mathbf{R} \nabla_{\mathbf{x}} \mathcal{H}(\mathbf{x}(t)))^\top \nabla_{\mathbf{x}} \mathcal{H}(\mathbf{x}(t))$ as power supply rate and power dissipation rate. By integration of (2) over a time period $[0, T]$, we arrive at the energy balance equation for pH systems

$$\mathcal{H}(\mathbf{x}(T)) - \mathcal{H}(\mathbf{x}(0)) = \int_{t=0}^T \mathbf{y}(t)^\top \mathbf{u}(t) dt - \int_{t=0}^T (\mathbf{R} \nabla_{\mathbf{x}} \mathcal{H}(\mathbf{x}(t)))^\top \nabla_{\mathbf{x}} \mathcal{H}(\mathbf{x}(t)) dt. \quad (3)$$

For more details on pH systems, we refer the reader to, e.g., [15, 30, 24, 18].

²We consider here state-independent system matrices \mathbf{J}, \mathbf{R} and \mathbf{B} for readability of the paper. Nevertheless, the in this paper presented MOR method also works for state-dependent system matrices.

2.2 Generalized manifold Galerkin

To ensure, that underlying structure in an initial value problem is preserved in the ROM, the paper [4] introduces a differential geometric framework. In this section, we recall the essential construction of the so-called *generalized manifold Galerkin* (GMG) reduction, introduced in the latter paper for, e.g., Hamiltonian and Lagrangian systems, since we will need this in the remainder of the paper to introduce our structure-preserving MOR method of pH systems. To stay within the notation of the paper, we denote the reduction map on a fixed chart and work with the representative matrices and vectors. For a formulation of the GMG reduction on manifolds, we refer the reader to [4, Section 5].

For our full order model (FOM), we consider an initial value problem of the form

$$\frac{d}{dt} \mathbf{x}(t) = \mathbf{f}(\mathbf{x}(t)) \quad \text{in } \mathbb{R}^N, t \in \mathcal{I}, \quad \mathbf{x}(t_0) = \mathbf{x}_0 \quad \text{in } \mathbb{R}^N,$$

with $\mathbf{f} : \mathbb{R}^N \rightarrow \mathbb{R}^N$. Our goal is to derive a ROM of form

$$\frac{d}{dt} \check{\mathbf{x}}(t) = \check{\mathbf{f}}(\check{\mathbf{x}}(t)) \quad \text{in } \mathbb{R}^r, t \in \mathcal{I}, \quad \check{\mathbf{x}}(t_0) = \check{\mathbf{x}}_0 \quad \text{in } \mathbb{R}^r, \quad (4)$$

where $\check{\mathbf{f}} : \mathbb{R}^r \rightarrow \mathbb{R}^r$, and $r \ll N$. To this end, we define an embedding and point reduction map by

$$\varphi : \mathbb{R}^r \rightarrow \mathbb{R}^N, \quad \rho : \mathbb{R}^N \rightarrow \mathbb{R}^r$$

satisfying a point projection property, i.e., $\rho \circ \varphi = \mathbb{1}_r$ for all $\check{\mathbf{x}} \in \mathbb{R}^r$, which leads to $\varphi \circ \rho$ being a point projection. To have a projection not only on the manifold itself, but additionally on the tangent bundle, we use the functions

$$D_{\check{\mathbf{x}}} \varphi : \mathbb{R}^r \rightarrow \mathbb{R}^N, \quad \mathcal{R}_{\text{red}, \check{\mathbf{x}}} : \mathbb{R}^N \rightarrow \mathbb{R}^r,$$

where $D_{\check{\mathbf{x}}} \varphi$ denotes the Jacobian of φ satisfying $\mathcal{R}_{\text{red}, \varphi(\check{\mathbf{x}})} \circ D_{\check{\mathbf{x}}} \varphi = \mathbb{1}_r$ for all $\check{\mathbf{x}} \in \mathbb{R}^r$, as tangent embedding and tangent reduction map, respectively. With these specification, we can define the quantities in (4) as the following

$$\check{\mathbf{f}}(\check{\mathbf{x}}) := \mathcal{R}_{\text{red}, \varphi(\check{\mathbf{x}})}(\mathbf{f}(\varphi(\check{\mathbf{x}}))) \quad \text{in } \mathbb{R}^r \quad \text{and} \quad \check{\mathbf{x}}_0 := \rho(\mathbf{x}_0).$$

With this setting, we are able to introduce the GMG reduction, which is a special kind of tangent reduction map that allows to preserve structure. We introduce the quantity encoding structure³ to be $\mathbf{G} \in \mathbb{R}^{N \times N}$ non-degenerate, which e.g., could be the canonical Poisson matrix in the reduction of Hamiltonian systems. Then, we define the *GMG reduction* by

$$\mathcal{R}_{\text{red}, \varphi(\check{\mathbf{x}})}(\mathbf{f}(\varphi(\check{\mathbf{x}}))) = \left((D_{\check{\mathbf{x}}} \varphi(\check{\mathbf{x}}))^{\top} \mathbf{G} D_{\check{\mathbf{x}}} \varphi(\check{\mathbf{x}}) \right)^{-1} (D_{\check{\mathbf{x}}} \varphi(\check{\mathbf{x}}))^{\top} \mathbf{G} \mathbf{f}(\varphi(\check{\mathbf{x}})).$$

We further denote the GMG reduction map in this paper by

$$\mathcal{F}_{\mathbf{G}}(D_{\check{\mathbf{x}}} \varphi(\check{\mathbf{x}})) = \left((D_{\check{\mathbf{x}}} \varphi(\check{\mathbf{x}}))^{\top} \mathbf{G} D_{\check{\mathbf{x}}} \varphi(\check{\mathbf{x}}) \right)^{-1} (D_{\check{\mathbf{x}}} \varphi(\check{\mathbf{x}}))^{\top} \mathbf{G}. \quad (5)$$

Here, we implicitly assume that $(D_{\check{\mathbf{x}}} \varphi(\check{\mathbf{x}}))^{\top} \mathbf{G} D_{\check{\mathbf{x}}} \varphi(\check{\mathbf{x}})$ is non-degenerate and for given M , we denote the set of all matrices satisfying this assumption by

$$\mathbf{S}_{\mathbf{G}} := \{ \mathbf{V} \in \mathbb{R}^{N \times r} \mid \det(\mathbf{V}^{\top} \mathbf{G} \mathbf{V}) \neq 0, 0 < r \leq N \}. \quad (6)$$

Although the GMG reduction provides a natural way of preserving structure in a ROM, it is not clear how to preserve the additional input-output structure of pH systems. We address this issue in Section 3.

2.3 Discrete empirical interpolation method for pH systems

We consider a nonlinear pH system $\Sigma(\mathbf{J}, \mathbf{R}, \mathcal{H}, \mathbf{B}, \mathbf{u}, \mathbf{y}, \mathbf{x}_0)$ where $\mathbf{J}, \mathbf{R}, \mathbf{B}$ are constant and \mathcal{H} is a nonlinear function. Even if a linear projection-based MOR method is used, the evaluation of the gradient of the reduced Hamiltonian involves quantities dependent on the FOM dimension, which is then not efficiently evaluable. The *discrete empirical interpolation method* (DEIM) [7] is an approach that overcomes this bottleneck by approximating the nonlinear terms via an interpolation. However, for port-Hamiltonian systems, the pH structure can be destroyed by applying DEIM. To ensure that the pH structure is being preserved, we use the structure-preserving DEIM introduced in [6], see also Algorithm 1. We summarize the procedure in the following.

³I.e., a matrix of component functions of (0,2)-tensor field, see again [4, Section 5].

We consider a nonlinear Hamiltonian $\mathcal{H}(x)$ and split it into two parts as follows

$$\mathcal{H}(x) = \frac{1}{2} x^\top \mathbf{Q} x + p(x), \quad p: \mathbb{R}^N \rightarrow \mathbb{R}, \quad \mathbf{Q} \succeq 0, \quad \mathbf{Q} = \mathbf{Q}^\top \in \mathbb{R}^{N \times N},$$

where \mathbf{Q} is the second order derivative of \mathcal{H} at an equilibrium point, i.e.

$$\mathbf{Q} = \frac{1}{2} \nabla_x^2 \mathcal{H}(x_e), \quad \nabla_x \mathcal{H}(x_e) = \mathbf{0}.$$

Further, we denote $q: \mathbb{R}^N \rightarrow \mathbb{R}^N$ by $q(x) = \nabla_x p(x)$. Then, a DEIM basis $\mathbf{U} = [\mathbf{u}_1, \dots, \mathbf{u}_d] \in \mathbb{R}^{N \times d}$ is built based on the POD basis of $[q(x(t_0)), \dots, q(x(t_{n_t}))] \in \mathbb{R}^{N \times (n_t+1)}$. After that, an index set $\{\xi_1, \dots, \xi_d\}$ where $\xi_i \in \{0, \dots, N\}$ is computed by using Algorithm 1, upon which an interpolation matrix $\mathbf{E} = [e_{\xi_1}, \dots, e_{\xi_d}] \in \mathbb{R}^{N \times d}$ is defined, where $e_i \in \mathbb{R}^N$ is the i -th column of \mathbb{I}_N , i.e., the identity matrix if size N . Subsequently, with the DEIM basis \mathbf{U} and the interpolation matrix \mathbf{E} , a DEIM approximation for q in $\text{span}(\mathbf{U})$ is given by

$$q(x) \approx \hat{q}(x) = \mathbb{P} q(\mathbb{P}^\top x), \quad \text{where } \mathbb{P} = \mathbf{U}(\mathbf{E}\mathbf{U})^{-1} \mathbf{E}^\top. \quad (7)$$

With this DEIM approximation, a DEIM Hamiltonian is defined by

$$\mathcal{H}_{\text{DEIM}}: x \rightarrow \frac{1}{2} x^\top \mathbf{Q} x + p(\mathbb{P}^\top x).$$

Algorithm 1 Structure-preserving DEIM for pH systems [6]

Input: Nonlinear Hamiltonian \mathcal{H} and an equilibrium point x_e , and DEIM size d .

Output: $\mathcal{H}_{\text{DEIM}}$.

- 1: Compute $\mathbf{Q} = \frac{1}{2} \nabla_x^2 \mathcal{H}(x_e)$, and denote $\nabla_x \mathcal{H}(x_e) = \mathbf{0}$.
 - 2: Construct a snapshot matrix by $[q(x(t_0)), \dots, q(x(t_{n_t}))]$.
 - 3: Build a DEIM basis $\mathbf{U}_d = [\mathbf{u}_1, \dots, \mathbf{u}_d] \in \mathbb{R}^{N \times d}$ based on the POD basis of this snapshot matrix.
 - 4: $[\rho, \xi_1] = \max\{|\mathbf{u}_1|\}$.
 - 5: **for** $\ell = 2$ to d **do**
 - 6: Solve $(\mathbf{E}^\top \mathbf{U}) \mathbf{c} = \mathbf{E}^\top \mathbf{u}_\ell$ for \mathbf{c} .
 - 7: $\mathbf{r} = \mathbf{U}_\ell - \mathbf{U} \mathbf{c}$.
 - 8: $[\rho, \xi_\ell] = \max\{|\mathbf{r}|\}$, where ξ_ℓ is given by the smallest index s.t. $|\mathbf{r}_{\xi_\ell}| = \max\{|\mathbf{r}|\}$.
 - 9: $\mathbf{U} \leftarrow [\mathbf{U}, \mathbf{u}_\ell]$, $\mathbf{E} \leftarrow [\mathbf{E}, e_{\xi_\ell}]$, $\xi \leftarrow [\xi^\top, \xi_\ell]^\top$.
 - 10: **end for**
 - 11: Denote $\mathbb{P} = \mathbf{U}(\mathbf{E}\mathbf{U})^{-1} \mathbf{E}^\top$.
 - 12: Define a DEIM Hamiltonian by $\mathcal{H}_{\text{DEIM}}: x \rightarrow \frac{1}{2} x^\top \mathbf{Q} x + p(\mathbb{P}^\top x)$.
-

3 Generalized manifold Galerkin for pH systems

We now detail how the structure-preserving MOR on manifolds of pH systems is performed based on the GMG reduction. To this end, we assume that we are given a pH system $\Sigma(\mathbf{J}, \mathbf{R}, \mathcal{H}, \mathbf{B}, \mathbf{u}, \mathbf{y}, x_0)$ (1). Then, our goal is to find an approximate solution

$$\tilde{x}(t) = \varphi(\check{x}(t)) \approx x(t), \quad (8)$$

where $\check{x}(t) \in \mathbb{R}^r$ is the reduced-order state, $\tilde{x}(t) \in \mathbb{R}^N$ is the reconstructed solution and $\varphi: \mathbb{R}^r \rightarrow \mathbb{R}^N$ with $m < r \ll N$ is a (possibly nonlinear) approximation map.

To derive a ROM we first define the time-continuous residual of the FOM (1) with respect to the reconstructed solution $\tilde{x}(t)$ by

$$\begin{aligned} \mathbf{r}(t) &:= \frac{d}{dt} \tilde{x}(t) - (\mathbf{J} - \mathbf{R}) \nabla_x \mathcal{H}(\tilde{x}(t)) - \mathbf{B} \mathbf{u}(t) \\ &= (\mathbf{D}_{\tilde{x}} \varphi(\check{x})) \frac{d}{dt} \check{x}(t) - (\mathbf{J} - \mathbf{R}) \nabla_x \mathcal{H}(\varphi(\check{x}(t))) - \mathbf{B} \mathbf{u}(t). \end{aligned}$$

Then, we require that by using the GMG reduction (5) the projected residual vanishes, i.e.,

$$\mathcal{W}(\check{x}(t))^\top \mathbf{r}(t) \stackrel{!}{=} \mathbf{0},$$

where we denote by $\mathcal{W}: \mathbb{R}^r \rightarrow \mathbb{R}^{N \times r}$ the GMG reduction map with

$$\mathcal{W}(\tilde{\mathbf{x}}) = \left(\mathcal{F}_{(\mathbf{J}-\mathbf{R})^{-1}}(\mathbf{D}_{\tilde{\mathbf{x}}}\varphi(\tilde{\mathbf{x}})) \right)^\top. \quad (9)$$

By reformulating the latter equation, we arrive at the following ROM

$$\frac{d}{dt}\tilde{\mathbf{x}}(t) = \mathcal{W}(\tilde{\mathbf{x}}(t))^\top (\mathbf{J} - \mathbf{R}) \nabla_{\mathbf{x}} \mathcal{H}(\varphi(\tilde{\mathbf{x}}(t))) + \mathcal{W}(\tilde{\mathbf{x}}(t))^\top \mathbf{B} \mathbf{u}(t), \quad (10a)$$

$$\dot{\mathbf{y}}(t) = \mathbf{B}^\top \nabla_{\mathbf{x}} \mathcal{H}(\varphi(\tilde{\mathbf{x}}(t))), \quad \tilde{\mathbf{x}}(0) = \tilde{\mathbf{x}}_0, \quad (10b)$$

where $\tilde{\mathbf{y}}(t) \in \mathbb{R}^m$ and the reduced initial condition is given by $\tilde{\mathbf{x}}_0 \in \mathbb{R}^r$. The following theorem discusses the conditions under which the ROM (10) is again a pH system.

Theorem 3.1. *Let $\Sigma(\mathbf{J}, \mathbf{R}, \mathcal{H}, \mathbf{B}, \mathbf{u}, \mathbf{y}, \mathbf{x}_0)$ be an N -dimensional pH system (1), and let $\varphi: \mathbb{R}^r \rightarrow \mathbb{R}^N$ be an approximation map. If for all $\tilde{\mathbf{x}} \in \mathbb{R}^r$, $\text{span}(\mathbf{B}) \subseteq \text{span}(\mathbf{D}_{\tilde{\mathbf{x}}}\varphi(\tilde{\mathbf{x}}))$ and $\mathbf{D}_{\tilde{\mathbf{x}}}\varphi(\tilde{\mathbf{x}}) \in \mathbf{S}_{(\mathbf{J}-\mathbf{R})^{-1}}$ (6), then the ROM obtained by using the GMG reduction in (10) is again a pH system.*

Proof. We have $\mathcal{V}: \tilde{\mathbf{x}} \mapsto \mathbf{D}_{\tilde{\mathbf{x}}}\varphi(\tilde{\mathbf{x}})$ and

$$\mathcal{W}: \tilde{\mathbf{x}} \mapsto \left(\mathcal{F}_{(\mathbf{J}-\mathbf{R})^{-1}}(\mathcal{V}(\tilde{\mathbf{x}})) \right)^\top,$$

such that $\mathcal{W}(\tilde{\mathbf{x}})^\top \mathcal{V}(\tilde{\mathbf{x}}) = \mathbb{I}_r$. By rearranging the terms in (10a), we arrive at (omitting state dependency in \mathcal{W}, \mathcal{V} for readability)

$$\begin{aligned} \frac{d}{dt}\tilde{\mathbf{x}}(t) &= \mathcal{W}^\top (\mathbf{J} - \mathbf{R}) \nabla_{\mathbf{x}} \mathcal{H}(\varphi(\tilde{\mathbf{x}}(t))) + \mathcal{W}^\top \mathbf{B} \mathbf{u}(t) \\ &= (\mathcal{V}^\top (\mathbf{J} - \mathbf{R})^{-1} \mathcal{V})^{-1} \mathcal{V}^\top (\mathbf{J} - \mathbf{R})^{-1} (\mathbf{J} - \mathbf{R}) \nabla_{\mathbf{x}} \mathcal{H}(\varphi(\tilde{\mathbf{x}}(t))) + \mathcal{W}^\top \mathbf{B} \mathbf{u}(t) \\ &= (\mathcal{V}^\top (\mathbf{J} - \mathbf{R})^{-1} \mathcal{V})^{-1} \mathcal{V}^\top \nabla_{\mathbf{x}} \mathcal{H}(\varphi(\tilde{\mathbf{x}}(t))) + \mathcal{W}^\top \mathbf{B} \mathbf{u}(t) \\ &= (\mathcal{V}^\top (\mathbf{J} - \mathbf{R})^{-1} \mathcal{V})^{-1} \nabla_{\tilde{\mathbf{x}}} \check{\mathcal{H}}(\tilde{\mathbf{x}}(t)) + \mathcal{W}^\top \mathbf{B} \mathbf{u}(t) \\ &= (\mathcal{V}^\top (\mathbf{J} - \mathbf{R})^{-1} \mathcal{V})^{-1} (\mathcal{V}^\top (\mathbf{J} - \mathbf{R})^{-\top} \mathcal{V}) (\mathcal{V}^\top (\mathbf{J} - \mathbf{R})^{-\top} \mathcal{V})^{-1} \nabla_{\tilde{\mathbf{x}}} \check{\mathcal{H}}(\tilde{\mathbf{x}}(t)) + \mathcal{W}^\top \mathbf{B} \mathbf{u}(t) \\ &= (\mathcal{V}^\top (\mathbf{J} - \mathbf{R})^{-1} \mathcal{V})^{-1} (\mathcal{V}^\top (\mathbf{J} - \mathbf{R})^{-\top} \mathcal{V}) (\mathcal{V}^\top (\mathbf{J} - \mathbf{R})^{-1} \mathcal{V})^{-\top} \nabla_{\tilde{\mathbf{x}}} \check{\mathcal{H}}(\tilde{\mathbf{x}}(t)) + \mathcal{W}^\top \mathbf{B} \mathbf{u}(t) \\ &= (\mathcal{V}^\top (\mathbf{J} - \mathbf{R})^{-1} \mathcal{V})^{-1} \mathcal{V}^\top (\mathbf{J} - \mathbf{R})^{-1} (\mathbf{J} - \mathbf{R}) (\mathbf{J} - \mathbf{R})^{-\top} \mathcal{V} (\mathcal{V}^\top (\mathbf{J} - \mathbf{R})^{-1} \mathcal{V})^{-\top} \nabla_{\tilde{\mathbf{x}}} \check{\mathcal{H}}(\tilde{\mathbf{x}}(t)) + \mathcal{W}^\top \mathbf{B} \mathbf{u}(t) \\ &= \mathcal{W}^\top (\mathbf{J} - \mathbf{R}) \mathcal{W} \nabla_{\tilde{\mathbf{x}}} \check{\mathcal{H}}(\tilde{\mathbf{x}}(t)) + \mathcal{W}^\top \mathbf{B} \mathbf{u}(t), \end{aligned}$$

where we define the reduced quantities naturally by

$$\check{\mathcal{J}}(\tilde{\mathbf{x}}) := \mathcal{W}(\tilde{\mathbf{x}})^\top \mathbf{J} \mathcal{W}(\tilde{\mathbf{x}}), \quad \check{\mathcal{R}}(\tilde{\mathbf{x}}) := \mathcal{W}(\tilde{\mathbf{x}})^\top \mathbf{R} \mathcal{W}(\tilde{\mathbf{x}}) \quad \text{and} \quad \check{\mathcal{H}}: \tilde{\mathbf{x}} \mapsto \mathcal{H}(\varphi(\tilde{\mathbf{x}})).$$

Note that $\check{\mathcal{J}}(\tilde{\mathbf{x}}) = -\check{\mathcal{J}}(\tilde{\mathbf{x}})^\top$, $\check{\mathcal{R}}(\tilde{\mathbf{x}}) = \check{\mathcal{R}}(\tilde{\mathbf{x}})^\top \geq 0$ and the reduced Hamiltonian $\check{\mathcal{H}}$ is continuously differentiable. However, for calling (10) a pH system, we still need to ensure that the output equation (10b) matches. Since $\text{span}(\mathbf{B}) \subseteq \text{span}(\mathcal{V}(\tilde{\mathbf{x}}))$, there exists a matrix $\mathbf{M} \in \mathbb{R}^{r \times m}$ such that $\mathbf{B} = \mathcal{V}(\tilde{\mathbf{x}}) \mathbf{M}$. Further, as $\mathcal{V}(\tilde{\mathbf{x}})^\top \mathcal{W}(\tilde{\mathbf{x}}) = \mathbb{I}_r$, we get

$$\mathbf{B}^\top = \mathbf{M}^\top \mathcal{V}(\tilde{\mathbf{x}})^\top = \mathbf{M}^\top \mathcal{V}(\tilde{\mathbf{x}})^\top \mathcal{W}(\tilde{\mathbf{x}}) \mathcal{V}(\tilde{\mathbf{x}})^\top = \mathbf{B}^\top \mathcal{W}(\tilde{\mathbf{x}}) \mathcal{V}(\tilde{\mathbf{x}})^\top. \quad (11)$$

Thus, we can rewrite (10b) by

$$\mathbf{B}^\top \nabla_{\mathbf{x}} \mathcal{H}(\varphi(\tilde{\mathbf{x}})) = \mathbf{B}^\top \mathcal{W}(\tilde{\mathbf{x}}) \mathcal{V}(\tilde{\mathbf{x}})^\top \nabla_{\mathbf{x}} \mathcal{H}(\varphi(\tilde{\mathbf{x}})) = \check{\mathcal{B}}(\tilde{\mathbf{x}})^\top \nabla_{\tilde{\mathbf{x}}} \check{\mathcal{H}}(\varphi(\tilde{\mathbf{x}})),$$

where we denote $\check{\mathcal{B}}(\tilde{\mathbf{x}}) := \mathcal{W}(\tilde{\mathbf{x}})^\top \mathbf{B} \in \mathbb{R}^{r \times m}$ and find that (10) is an r -dimensional pH system which can be described by $\Sigma(\check{\mathcal{J}}(\tilde{\mathbf{x}}), \check{\mathcal{R}}(\tilde{\mathbf{x}}), \check{\mathcal{H}}, \check{\mathcal{B}}(\tilde{\mathbf{x}}), \mathbf{u}, \dot{\mathbf{y}}, \tilde{\mathbf{x}}_0)$. \square

4 State approximation and corresponding ROMs

In this section, we discuss how to construct the approximation map φ (8) such that the requirements from Theorem 3.1 are fulfilled naturally by construction and discuss specific realizations. To this end, we start with the following form of φ

$$\varphi(\tilde{\mathbf{x}}) = \mathbf{B} \tilde{\mathbf{x}}_1 + \overline{\mathbf{V}} \eta(\tilde{\mathbf{x}}_2), \quad \tilde{\mathbf{x}}_1 \in \mathbb{R}^m, \quad \tilde{\mathbf{x}}_2 \in \mathbb{R}^{r-m}, \quad \tilde{\mathbf{x}} = \begin{bmatrix} \tilde{\mathbf{x}}_1 \\ \tilde{\mathbf{x}}_2 \end{bmatrix}, \quad (12)$$

with matrix $\bar{V} \in \mathbb{R}^{N \times (r_n+r-m)}$ satisfying $B^\top \bar{V} = \mathbf{0}_{m \times (r_n+r-m)}$, and $\eta \in C^1(\mathbb{R}^{r-m}, \mathbb{R}^{r_n+r-m})$ with the dimension $0 \leq r_n \ll N$ being identified for each concrete realization of η . While η could be any general nonlinear map, such as e.g., a neural network, we consider a linear and quadratic approximation map in this paper, and detail their choice and the resulting ROMs in Section 4.2. We start by showing that the assumptions Theorem 3.1 are satisfied for the general representation of φ in (12).

4.1 Constructing pH systems with state approximation

Theorem 3.1 shows that the GMG reduction map preserves the pH structure if the approximation map satisfies that (i) $\text{span}(B) \subseteq \text{span}(D_{\check{x}}\varphi(\check{x}))$ and (ii) $D_{\check{x}}\varphi(\check{x}) \in \mathbf{S}_{(\mathbf{J}-R)^{-1}}$. We note, that due to the special structure of the approximation map (12), we arrive at the Jacobian $D_{\check{x}}\varphi(\check{x}) = [B, \bar{V}D_{\check{x}_2}\eta(\check{x}_2)] \in \mathbb{R}^{N \times r}$, such that condition (i), i.e., $\text{span}(B) \subseteq \text{span}(D_{\check{x}}\varphi(\check{x}))$ is automatically satisfied. Moreover, with this construction, we arrive at \check{B} being a constant function given by $\check{B}: \check{x} \mapsto \begin{bmatrix} \mathbb{1}_m \\ \mathbf{0}_{r-m,m} \end{bmatrix}$, which follows from $B^\top = \mathcal{V}(\check{x})\mathcal{W}(\check{x})^\top B$, see (11) and $\text{span}(B) \subseteq \text{span}(D_{\check{x}}\varphi(\check{x}))$.

4.2 State-approximations and resulting ROMs

To determine the unknown matrices/function of the approximation map φ , we use a data-driven approach. To this end, we introduce an equidistant time discretization of the time interval $(t_0, t_{\text{end}}]$ with $\Delta t := (t_{\text{end}} - t_0)/n_t$, $n_t \in \mathbb{N}$. Then, for $t_i := t_0 + i\Delta t$, $0 \leq i \leq n_t$, we seek approximations $\mathbf{x}^i \approx \mathbf{x}(t_i)$, $\mathbf{y}^i \approx \mathbf{y}(t_i)$. We query the pH system (1) to obtain a so-called *snapshot matrix*

$$\mathbf{X} := [\mathbf{x}^0, \dots, \mathbf{x}^{n_t}] \in \mathbb{R}^{N \times (n_t+1)}. \quad (13)$$

In the following, we state particular cases of approximation map (8) such that it results (i) into a linear (Section 4.2.1) and (ii) into a quadratic map (Section 4.2.2).

4.2.1 Linear state approximation and GMG-POD-ROM

We here choose η to be the identity map on \mathbb{R}^{r-m} , i.e., $\eta: \mathbb{R}^{r-m} \rightarrow \mathbb{R}^{r-m}$. Then, the formulation in (12) results in a linear approximation map

$$\varphi_{\text{lin}}(\check{x}) = \mathbf{V}\check{x} = \mathbf{B}\check{x}_1 + \bar{\mathbf{V}}\check{x}_2, \quad (14)$$

with $\mathbf{V} = [B, \bar{V}] \in \mathbb{R}^{N \times r}$, where we assume, that \mathbf{V} has full column rank. This is a weak assumption as we can ensure full column rank of \bar{V} by construction and in case that B is not of full column rank, the pH system can be rewritten in a form with less ports. Further, as B is given by the problem formulation, we only need to find a suitable \bar{V} such that the conditions of Theorem 3.1 are fulfilled. This is done via the following optimization where $(\cdot)^\dagger$ represents the Moore-Penrose pseudo inverse

$$\begin{aligned} \bar{V} &= \underset{A \in \Xi_{\bar{V}}}{\text{argmin}} \sum_{i=0}^{n_t} \left\| \mathbf{x}^i - [B, A] [B, A]^\dagger \mathbf{x}^i \right\|_2^2 \\ &= \underset{A \in \Xi_{\bar{V}}}{\text{argmin}} \left\| \mathbf{X} - [B, A] [B, A]^\dagger \mathbf{X} \right\|_F^2 \\ &= \underset{A \in \Xi_{\bar{V}}}{\text{argmin}} \left\| \mathbf{X} - \mathbf{B}\mathbf{B}^\dagger \mathbf{X} - \mathbf{A}\mathbf{A}^\dagger \mathbf{X} \right\|_F^2 \\ &= \underset{A \in \Xi_{\bar{V}}}{\text{argmin}} \left\| \mathbf{X} - \mathbf{B}\mathbf{B}^\dagger \mathbf{X} - \mathbf{A}\mathbf{A}^\top \mathbf{X} + \mathbf{A}\mathbf{A}^\top \mathbf{B}\mathbf{B}^\dagger \mathbf{X} \right\|_F^2 \\ &= \underset{A \in \Xi_{\bar{V}}}{\text{argmin}} \left\| (\mathbb{1}_N - \mathbf{A}\mathbf{A}^\top)(\mathbf{X} - \mathbf{B}\mathbf{B}^\dagger \mathbf{X}) \right\|_F^2, \end{aligned}$$

where $\Xi_{\bar{V}} = \{A \mid A \in \mathbb{R}^{N \times (r-m)}, B^\top A = \mathbf{0}_{m \times (r-m)}, A^\top A = \mathbb{1}_{r-m}\}$. This means, that we can determine \bar{V} by the POD over the adjusted snapshot matrix $\mathbf{X} - \mathbf{B}\mathbf{B}^\dagger \mathbf{X}$. For the point reduction map, which is used to map the initial condition, we choose

$$\rho_{\text{lin}}(\mathbf{x}) := \mathbf{V}^\dagger \mathbf{x} = \begin{bmatrix} B^\dagger, & \bar{V}^\top \end{bmatrix}^\top \mathbf{x}, \quad (15)$$

which has been used already in the derivations made above, such that the point projection property, i.e., $\rho_{\text{lin}} \circ \varphi_{\text{lin}} = \text{id}_{\mathbb{R}^r}$ is fulfilled. The resulting ROM from the choice of φ_{lin} , ρ_{lin} and the corresponding GMG reduction is called GMG-POD-ROM. We describe the procedure in pseudo-code in Algorithm 2. Additionally, as we investigate nonlinear pH systems in the numerical experiments in this paper, we include the DEIM approximation introduced in Section 2.3 in the algorithm.

Algorithm 2 GMG-POD-ROM (with DEIM)

Input: pH system $\Sigma(\mathbf{J}, \mathbf{R}, \mathcal{H}, \mathbf{B}, \mathbf{u}, \mathbf{y}, \mathbf{x}_0)$, reduced order $r > m$, DEIM tolerance ϵ_{DEIM} , and time discretization $[t_0, \dots, t_{n_t}]$.

Output: reduced order pH system $\Sigma(\check{\mathbf{J}}, \check{\mathbf{R}}, \check{\mathcal{H}}, \check{\mathbf{B}}, \mathbf{u}, \check{\mathbf{y}}, \check{\mathbf{x}}_0)$

- 1: Find an equilibrium point $\mathbf{x}_e \in \mathbb{R}^N$ of \mathcal{H} such that $\nabla_{\mathbf{x}_e} \mathcal{H}(\mathbf{x}_e) = \mathbf{0}$.
- 2: Compute $\mathbf{Q} \in \mathbb{R}^{N \times N}$ by $\mathbf{Q} = \frac{1}{2} \nabla_{\mathbf{x}_e}^2 \mathcal{H}(\mathbf{x}_e)$.
- 3: Set $q: \mathbf{x} \mapsto \nabla_{\mathbf{x}} \mathcal{H}(\mathbf{x}) - \mathbf{Q}\mathbf{x}$, and $p: \mathbf{x} \mapsto \mathcal{H}(\mathbf{x}) - \frac{1}{2} \mathbf{x}^\top \mathbf{Q}\mathbf{x}$.
- 4: Run the simulation of the FOM with the given time discretization and denote

$$\mathbf{X} = [\mathbf{x}^0, \dots, \mathbf{x}^{n_t}], \quad \mathbf{X}_Q = [q(\mathbf{x}^0), \dots, q(\mathbf{x}^{n_t})].$$

- 5: Build DEIM basis $\mathbf{U}_{\text{DEIM}} \in \mathbb{R}^{N \times d}$ based on \mathbf{X}_Q s.t.

$$\frac{\|\mathbf{X}_Q - \mathbf{U}_{\text{DEIM}} \mathbf{U}_{\text{DEIM}}^\top \mathbf{X}_Q\|_F}{\|\mathbf{X}_Q\|_F} < \epsilon_{\text{DEIM}}, \quad (16)$$

where d is selected as the minimal integer such that (16) holds.

- 6: Compute DEIM indices ξ by Algorithm 1, and build the DEIM approximation \mathbb{P} by (7).
- 7: Build $\bar{\mathbf{V}}$ by the first $r - m$ left singular vectors of $\mathbf{X} - \mathbf{B}\mathbf{B}^\dagger \mathbf{X}$.
- 8: Assemble $\mathbf{V} = [\mathbf{B}, \bar{\mathbf{V}}]$.
- 9: Build the reduction map presented in (9), where \mathbf{W} results in

$$\mathbf{W} = (\mathcal{F}_{(\mathbf{J}-\mathbf{R})^{-1}}(\mathbf{V}))^\top = (\mathbf{J} - \mathbf{R})^{-\top} \mathbf{V} (\mathbf{V}^\top (\mathbf{J} - \mathbf{R})^{-1} \mathbf{V})^{-\top}.$$

- 10: Construct reduced-order pH system $\Sigma(\check{\mathbf{J}}, \check{\mathbf{R}}, \check{\mathcal{H}}, \check{\mathbf{B}}, \mathbf{u}, \check{\mathbf{y}}, \check{\mathbf{x}}_0)$ with

$$\begin{aligned} \check{\mathbf{J}} &= \mathbf{W}^\top \mathbf{J} \mathbf{W}, \quad \check{\mathbf{B}} = [\mathbb{1}_m, \mathbf{0}]^\top, \quad \check{\mathbf{R}} = \mathbf{W}^\top \mathbf{R} \mathbf{W}, \\ \check{\mathcal{H}}(\check{\mathbf{x}}) &= \frac{1}{2} \check{\mathbf{x}}^\top \mathbf{V}^\top \mathbf{Q} \mathbf{V} \check{\mathbf{x}} + p(\mathbb{P}^\top \mathbf{V} \check{\mathbf{x}}), \quad \check{\mathbf{x}}_0 = \mathbf{V}^\dagger \mathbf{x}. \end{aligned}$$

4.2.2 Quadratic state approximation and GMG-QM-ROM

In this section, we consider approximations φ on quadratically embedded manifolds, i.e.,

$$\varphi_{\text{quad}}(\check{\mathbf{x}}) = \mathbf{B}\check{\mathbf{x}}_1 + \bar{\mathbf{V}}_1 \check{\mathbf{x}}_2 + \bar{\mathbf{V}}_2 \mathbf{M}(\check{\mathbf{x}}_2 \otimes \check{\mathbf{x}}_2), \quad \check{\mathbf{x}}_1 \in \mathbb{R}^m, \quad \check{\mathbf{x}}_2 \in \mathbb{R}^{r-m}, \quad (17)$$

where $r_n \leq (r - m)^2$ is a lifting order, \otimes denotes the Kronecker product, $\bar{\mathbf{V}}_1 \in \mathbb{R}^{N \times (r-m)}$, $\bar{\mathbf{V}}_2 \in \mathbb{R}^{N \times r_n}$ and $\mathbf{M} \in \mathbb{R}^{r_n \times (r-m)^2}$. In the following, we would like to discuss how to construct $\bar{\mathbf{V}}_1$, $\bar{\mathbf{V}}_2$ and \mathbf{M} . First, we build $\bar{\mathbf{V}}_1$ and $\bar{\mathbf{V}}_2$ by the POD basis of $\mathbf{X} - \mathbf{B}\mathbf{B}^\dagger \mathbf{X}$, where $\mathbf{X} \in \mathbb{R}^{N \times n_t}$ is the snapshot matrix (13), s.t.

$$\bar{\mathbf{V}}_1 = \underset{\mathbf{A} \in \mathbb{R}^{N \times (r-m)}, \mathbf{A}^\top \mathbf{A} = \mathbb{1}_{r-m}}{\text{argmin}} \left\| (\mathbb{1}_N - \mathbf{A}\mathbf{A}^\top)(\mathbf{X} - \mathbf{B}\mathbf{B}^\dagger \mathbf{X}) \right\|_F^2, \quad \text{and} \quad (18)$$

$$\bar{\mathbf{V}}_2 = \underset{\mathbf{A} \in \mathbb{R}^{N \times r_n}, \mathbf{A}^\top \mathbf{A} = \mathbb{1}_{r_n}}{\text{argmin}} \left\| (\mathbb{1}_N - \mathbf{A}\mathbf{A}^\top)(\mathbf{X} - [\mathbf{B}, \bar{\mathbf{V}}_1][\mathbf{B}, \bar{\mathbf{V}}_1]^\dagger \mathbf{X}) \right\|_F^2. \quad (19)$$

Then, we construct \mathbf{M} based on the solution of the following optimization problem:

$$\underset{\mathbf{A} \in \mathbb{R}^{r_n \times (r-m)^2}}{\text{argmin}} \sum_{i=1}^{n_t} \min_{\check{\mathbf{x}}_1 \in \mathbb{R}^m, \check{\mathbf{x}}_2 \in \mathbb{R}^{r-m}} \left\| \mathbf{x}^i - \mathbf{B}\check{\mathbf{x}}_1 - \bar{\mathbf{V}}_1 \check{\mathbf{x}}_2 - \bar{\mathbf{V}}_2 \mathbf{A}(\check{\mathbf{x}}_2 \otimes \check{\mathbf{x}}_2) \right\|_2^2. \quad (20)$$

We now detail how M this can be computed. Note, that

$$\sum_{i=1}^{n_t} \min_{\tilde{x}_1 \in \mathbb{R}^m, \tilde{x}_2 \in \mathbb{R}^{r-m}} \left\| x^i - B\tilde{x}_1 - \bar{V}_1 \tilde{x}_2 \right\|_2^2 = \sum_{i=1}^{n_t} \|r_{QM}^i\|_2^2,$$

where $r_{QM}^i := x^i - BB^\top x^i - \bar{V}_1 \bar{V}_1^\top x^i$. Thus, we approximate (20) by

$$\operatorname{argmin}_{A \in \mathbb{R}^{r_n \times (r-m)^2}} \sum_{i=1}^{n_t} \left\| r_{QM}^i - A(x_2^i \otimes x_2^i) \right\|_2^2, \quad (21)$$

where $x_2^i = \bar{V}_1^\top x^i$. Based on (21), we arrive at matrix M given by the solution of the least squares problem

$$\operatorname{argmin}_{A \in \mathbb{R}^{r_n \times (r-m)^2}} \left(\sum_{i=1}^{n_t} \left\| r_{QM}^i - A(x_2^i \otimes x_2^i) \right\|_2^2 + \lambda_{\text{reg}} \|A\|_F^2 \right), \quad (22)$$

where $\lambda_{\text{reg}} \in \mathbb{R}^+$ is a regularization parameter. We use the same point reduction used in GMG-POD-ROM, i.e., $\rho_{\text{quad}}(x) = [B, \bar{V}_1]^\top x$. From (19), we have $\bar{V}_2 \perp [B, \bar{V}_1]$, which ensures that the point reduction property is satisfied, i.e., $\rho_{\text{quad}} \circ \varphi_{\text{quad}} = \text{id}_{\mathbb{R}^r}$. The resulting ROM obtained by φ_{quad} , ρ_{quad} and the corresponding GMG reduction map is again a pH system, and We denote it by GMG-QM-ROM. A pseudo-code that describes this procedure is given in Algorithm 3.

Algorithm 3 GMG-QM-ROM (with DEIM)

Input: pH system $\Sigma(J, R, \mathcal{H}, B, u, y, x_0)$, reduced order $r > m$, DEIM tolerance ϵ_{DEIM} , regularization parameter λ_{reg} , dimension r_n .

Output: A reduced order pH system $\Sigma(\check{J}(\check{x}), \check{R}(\check{x}), \check{\mathcal{H}}, \check{B}, u, \check{y}, \check{x}_0)$

1-5: Same as Steps 1–5 of Algorithm 2.

6: Construct \bar{V}_1 and \bar{V}_2 by (18) and (19).

7: Compute M by (22), and build the approximation function φ by (17).

8: Denote $\mathcal{V}: \check{x} \mapsto D_{\check{x}}\varphi(\check{x})$, and construct the GMG reduction by

$$\mathcal{W}: \check{x} \mapsto (\mathcal{F}_{(J-R)^{-1}}(\mathcal{V}(\check{x})))^\top.$$

9: Construct the reduced-order pH system $\Sigma(\check{J}(\check{x}), \check{R}(\check{x}), \check{\mathcal{H}}, \check{B}, u, \check{y}, \check{x}_0)$, where

$$\begin{aligned} \check{J}(\check{x}) &= \mathcal{W}(\check{x})^\top J(\varphi(\check{x})) \mathcal{W}(\check{x}), & \check{R}(\check{x}) &= \mathcal{W}(\check{x})^\top R(\varphi(\check{x})) \mathcal{W}(\check{x}), \\ \check{\mathcal{H}}(\check{x}) &= \frac{1}{2} \varphi(\check{x})^\top Q \varphi(\check{x}) + p(\mathbb{P}^\top \varphi(\check{x})), & \check{B} &= [0_m, \mathbf{0}_{m, r-m}], & \check{x}_0 &= [B, \bar{V}_1]^\top x_0. \end{aligned}$$

5 Numerical results

In this section, we perform numerical experiments on two systems and compare the performance of the MOR methods introduced in Section 4.2.1 and 4.2.2 compared to existing MOR methods of pH systems. In Section 5.1 we provide implementation details and introduce error measures used in the subsequent section. A linear mass-spring-damper system is used as example in Section 5.2, and a nonlinear mass-spring-damper system is investigated in Section 5.3.

5.1 Implementation details and error measures

In this paper, all numerical simulations are conducted using Python version 3.11. For the temporal integration in all simulations, we use the Gauss-Legendre method of order 6 as it preserves the pH structure [17]. If the pH system is nonlinear, the time integration method is implicit and it is computed using Newton's method at every time step. We compare our introduced MOR methods of pH systems to existing structure-preserving MOR methods known from the literature. For the comparison of the linear mass-spring-damper system, we use the method introduced in [27], for which we call the resulting reduced order model SP1-POD-ROM. While the nonlinear mass-spring-damper system involves a nonlinear Hamiltonian, we compare our results to the structure-preserving

MOR method presented in , for which we call the resulting reduced order model SP2-POD-ROM. We briefly recall both methods in the following.

The SP1-POD-ROM uses a linear approximation $\varphi: \tilde{\mathbf{x}} \mapsto \mathbf{V}_{\text{POD}}\tilde{\mathbf{x}}$ with $\mathbf{V}_{\text{POD}} \in \mathbb{R}^{N \times r}$ constructed by the first r modes of the POD basis of the snapshots \mathbf{X} (13), i.e.,

$$\mathbf{V}_{\text{POD}} = \underset{\mathbf{A}^\top \mathbf{A} = \mathbf{I}_r}{\text{argmin}} (\|\mathbf{X} - \mathbf{A}\mathbf{A}^\top \mathbf{X}\|_F). \quad (23)$$

Then, the reduction map $\mathcal{R}_{\text{red}}: \mathbf{x} \mapsto \mathbf{W}\mathbf{x}$ is built with $\mathbf{W} \in \mathbb{R}^{N \times r}$ constructed by a GMG reduction with matrix \mathbf{Q}

$$\mathbf{W} = \mathcal{F}_Q(\mathbf{V}_{\text{POD}})^\top = \mathbf{Q}\mathbf{V}(\mathbf{V}^\top \mathbf{Q}\mathbf{V})^{-1}, \quad (24)$$

where $\mathbf{Q} = \nabla_{\mathbf{x}}^2 \mathcal{H}$ is the Hessian matrix of a quadratic Hamiltonian. The same linear approximation map is used in SP2-POD. However, a different reduction map is applied. First, a matrix $\mathbf{V}_{\nabla_{\mathbf{x}} \mathcal{H}} \in \mathbb{R}^{N \times r}$ is constructed by the first r modes of the POD basis of $\mathbf{X}_{\nabla_{\mathbf{x}} \mathcal{H}}$, where $\mathbf{X}_{\nabla_{\mathbf{x}} \mathcal{H}} := [\nabla_{\mathbf{x}} \mathcal{H}(\mathbf{x}^0), \dots, \nabla_{\mathbf{x}} \mathcal{H}(\mathbf{x}^{n_t})]$ is the snapshots matrix of the gradient of the Hamiltonian. Then, a linear reduction map $\mathcal{R}_{\text{red}}: \mathbf{x} \mapsto \mathbf{W}\mathbf{x}$ is built with $\mathbf{W} \in \mathbb{R}^{N \times r}$ given by

$$\mathbf{W} = (\mathbf{V}_{\nabla_{\mathbf{x}} \mathcal{H}}^\top \mathbf{V}_{\text{POD}})^{-1} \mathbf{V}_{\nabla_{\mathbf{x}} \mathcal{H}}. \quad (25)$$

To summarize and clarify the differences between these methods, the resulting ROMs with the corresponding approximation and reduction maps are listed in Table 1

ROM	Approximation map $\varphi: \tilde{\mathbf{x}} \mapsto$	Reduction map $\mathcal{R}_{\text{red}, \varphi(\tilde{\mathbf{x}}): \mathbf{x} \mapsto$
SP1-POD-ROM [27]	$\mathbf{V}_{\text{POD}}\tilde{\mathbf{x}}$ (23)	$\mathcal{F}_Q(\mathbf{V}_{\text{POD}})^\top \mathbf{x}$ (24)
SP2-POD-ROM [6]	$\mathbf{V}_{\text{POD}}\tilde{\mathbf{x}}$ (23)	$(\mathbf{V}_{\nabla_{\mathbf{x}} \mathcal{H}}^\top \mathbf{V}_{\text{POD}})^{-1} \mathbf{V}_{\nabla_{\mathbf{x}} \mathcal{H}} \mathbf{x}$ (25)
GMG-POD-ROM	$[\mathbf{B}, \overline{\mathbf{V}}] \tilde{\mathbf{x}}$ (14)	$\mathcal{F}_{(\mathbf{J}-\mathbf{R})^{-1}}(\mathbf{D}_{\tilde{\mathbf{x}}} \varphi(\tilde{\mathbf{x}}))^\top \mathbf{x}$ (9)
GMG-QM-ROM	$\mathbf{B}\tilde{\mathbf{x}}_1 + \overline{\mathbf{V}}_1 \tilde{\mathbf{x}}_1 + \overline{\mathbf{V}}_2 \mathbf{M}\tilde{\mathbf{x}}_2 \otimes \tilde{\mathbf{x}}_2$ (17)	$\mathcal{F}_{(\mathbf{J}-\mathbf{R})^{-1}}(\mathbf{D}_{\tilde{\mathbf{x}}} \varphi(\tilde{\mathbf{x}}))^\top \mathbf{x}$ (9)

Table 1: Approximation and reduction maps of different MOR methods and resulting ROMs.

To compare the performance of these MOR methods, we introduce error measures with respect to the state, the output and how well the energy balance equation is fulfilled. Assume we have trajectories of the FOM and ROMs given by $[\mathbf{x}^0, \dots, \mathbf{x}^{n_t}]$ and $[\tilde{\mathbf{x}}(t_0), \dots, \tilde{\mathbf{x}}(t_{n_t})]$ respectively. We denote the relative reduced and projection error of the state by $e_{\mathbf{x}, \text{red}}$, and $e_{\mathbf{x}, \text{proj}}$ given by

$$e_{\mathbf{x}, \text{red}} = \sqrt{\frac{\sum_{i=1}^{n_t} \|\mathbf{x}^i - \varphi(\tilde{\mathbf{x}}(t_i))\|_2^2}{\sum_{i=1}^{n_t} \|\mathbf{x}^i\|_2^2}}, \quad (26)$$

$$e_{\mathbf{x}, \text{proj}} = \sqrt{\frac{\sum_{i=1}^{n_t} \|\mathbf{x}^i - \varphi(\rho(\mathbf{x}^i))\|_2^2}{\sum_{i=1}^{n_t} \|\mathbf{x}^i\|_2^2}}. \quad (27)$$

For a nonlinear map of the form of φ in (17), we can compute a lower bound presented in [3] for its reduction error given by

$$e_{\mathbf{x}, \text{lowerbound}} = \sqrt{\left(\sum_{i=1}^{n_t} \left\| (\mathbf{I} - \mathbf{B}\mathbf{B}^\top - \overline{\mathbf{V}}_1 \overline{\mathbf{V}}_1^\top - \overline{\mathbf{V}}_2 \overline{\mathbf{V}}_2^\top) \mathbf{x}^i \right\|_2^2 \right) \left(\sum_{i=1}^{n_t} \|\mathbf{x}^i\|_2^2 \right)}. \quad (28)$$

The average relative output error is computed by

$$e_{\mathbf{y}} = \sqrt{\frac{\sum_{i=1}^{n_t} \|\mathbf{y}^i - \tilde{\mathbf{y}}(t_i)\|_2^2}{\sum_{i=1}^{n_t} \|\mathbf{y}^i\|_2^2}}, \quad (29)$$

where \mathbf{y} and $\tilde{\mathbf{y}}$ are outputs of the FOM and the ROM. Furthermore, we evaluate how well the energy balance equation (3) is preserved by the MOR methods. We denote this error by

$$\text{error}_{\text{energy}}(T) := \left| \mathcal{H}(\mathbf{x}(T)) - \mathcal{H}(\mathbf{x}(0)) - \int_{t=0}^T \mathbf{y}(t)^\top \mathbf{u}(t) dt + \int_{t=0}^T (\mathbf{R}\nabla_{\mathbf{x}} \mathcal{H}(\mathbf{x}(t)))^\top \nabla_{\mathbf{x}} \mathcal{H}(\mathbf{x}(t)) dt \right|. \quad (30)$$

5.2 Linear mass-spring-damper system

We test a linear mass-spring-damper system, see e.g., [12], depicted in Figure 1. For $i = 1, \dots, \frac{N}{2} - 1$, the masses m_i and m_{i+1} are connected by a spring with stiffness coefficient k_i . The last mass block $m_{\frac{N}{2}}$ is connected to a wall with a spring stiffness coefficient $k_{\frac{N}{2}}$. Dampers are applied to all masses, and the damper coefficient associated with mass m_i is c_i for $i = 1, \dots, \frac{N}{2}$.

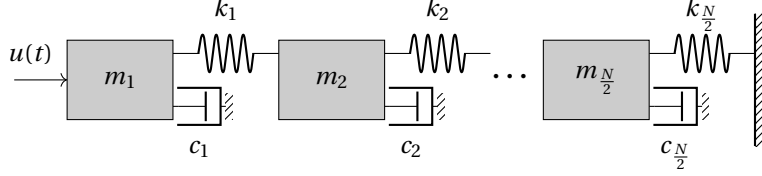


Figure 1: Linear mass-spring-damper system

A realization of this system for order $n = 6$ is

$$B = \begin{bmatrix} 0 \\ 1 \\ 0 \\ 0 \\ 0 \\ 0 \end{bmatrix}, \quad J = \begin{bmatrix} \mathbf{J}_2 & \mathbf{0} & \mathbf{0} \\ \mathbf{0} & \mathbf{J}_2 & \mathbf{0} \\ \mathbf{0} & \mathbf{0} & \mathbf{J}_2 \end{bmatrix}, \quad R = \text{diag}(0, c_1, 0, c_2, 0, c_3),$$

$$\mathcal{H}: x \mapsto \frac{1}{2} x^\top Q x, \quad \text{with } Q = \begin{bmatrix} k_1 & 0 & -k_1 & 0 & 0 & 0 \\ 0 & \frac{1}{m_1} & 0 & 0 & 0 & 0 \\ -k_1 & 0 & k_1 + k_2 & 0 & -k_2 & 0 \\ 0 & 0 & 0 & \frac{1}{m_2} & 0 & 0 \\ 0 & 0 & -k_2 & 0 & k_2 + k_3 & 0 \\ 0 & 0 & 0 & 0 & 0 & \frac{1}{m_3} \end{bmatrix},$$

where $\mathbf{J}_2 = \begin{bmatrix} 0 & 1 \\ -1 & 0 \end{bmatrix}$ is the two-dimensional canonical Poisson matrix. We consider an 100-dimensional mass-spring-damper system where $m_i = 2$, $k_i = 1$, and $c_i = 1$ for $i = 1, 2, \dots, 50$. The time interval $(0, 100\text{s}]$ is discretized with a uniform discretization step given by $\Delta t = 0.1\text{s}$, resulting in $n_t = 1001$. We consider two different inputs $u(t) = 0.1$ and $u(t) = 0.1 \sin(t)$. For the GMG-QM-ROM, we set $r_n = 8$, and $\lambda_{\text{reg}} = 10^{-3}$. The tolerance and maximum number of iterations of the Newton's method are set to 10^{-10} and 10.

In Figure 2a and 2b, the relative reduction and projection error of the state are shown. These results show that the ROMs based in the GMG projection-based MOR methods introduced in this paper achieve higher accuracy compared to the SP1-POD-ROM. Further, the GMG-QM-ROM outperforms the GMG-POD-ROM as a quadratic approximation map is applied. For the GMG-POD-ROM methods, the reduction error is just slightly above the projection error. Furthermore, the quadratic reduced error is close to its lower bound (28). The comparison of the output error can be found in Figure 2c and 2d. The results show a similar trend to the state error. The GMG projection-based methods have better accuracy compared to the SP1-POD, while the GMG-QM-ROM performs better than the GMG-POD-ROM.

5.3 Nonlinear mass-spring-damper system

For the second numerical example, we consider a nonlinear mass-spring-damper system that consists of n masses. This problem is similar to [1, Section 5.2.2].

A nonlinear spring and a linear damper are connected between the mass m_i and mass m_{i+1} for $i = 1, \dots, n - 1$. The spring and damper coefficients are $k_1 + k_2(\xi_{i+1} - \xi_i)^2$ and γ_i , where ξ_i is the position of the mass m_i . The last mass is connected to the wall with a linear spring and a linear damper where the spring coefficient and the damper coefficient are $k_1 + k_2\xi_n^2$ and γ_n . We denote $x = [x_1, \dots, x_N]^\top = [\xi, \dots, \xi_n, \dot{\xi}_1, \dots, \dot{\xi}_n]^\top$ as the state, and we get a pH

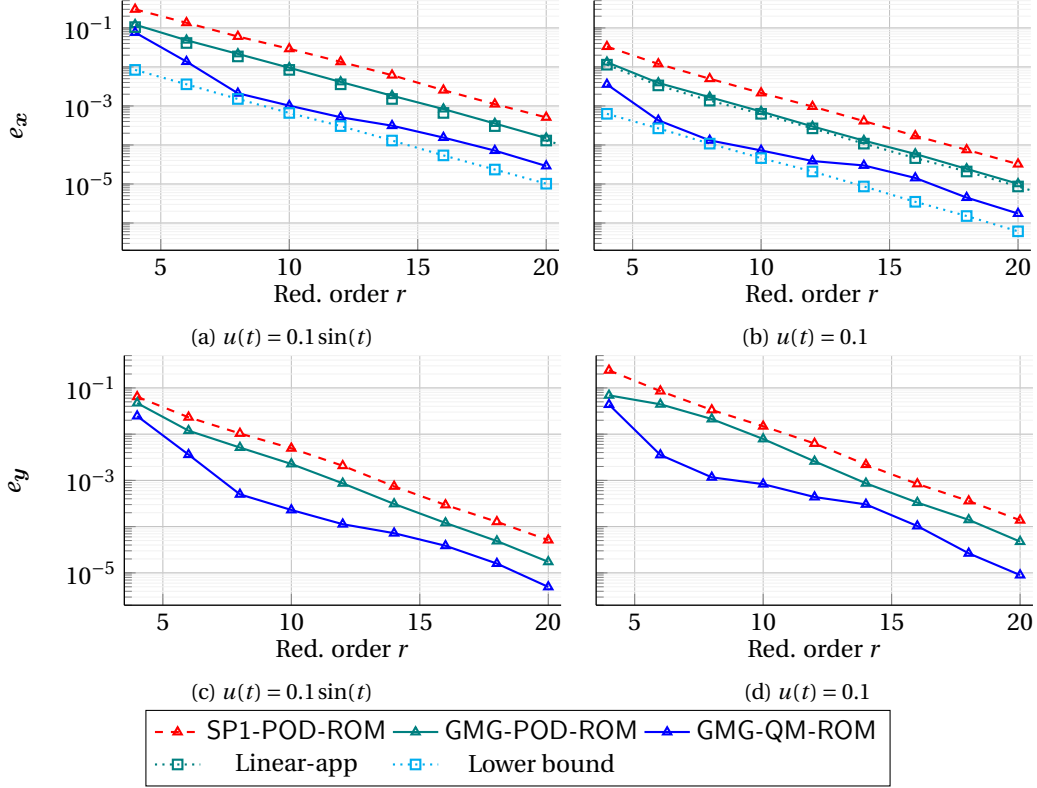


Figure 2: Reduction and output error obtained by SP1-POD-ROM, GMG-POD-ROM, and GMG-QM-ROM for the linear mass-spring-damper system with the inputs $u(t) = 0.1$ and $u(t) = 0.1 \sin(t)$. Linear-app represents the projection error of corresponding linear embedding maps. The lower bound for the ROMs resulting from the quadratic embeddings maps is computed by (28).

modelling of this system given by $\Sigma(J, \mathbf{R}, \mathcal{H}, \mathbf{B}, \mathbf{u}, \mathbf{y}, \mathbf{x}_0)$ where

$$\mathbf{B} = \begin{bmatrix} \mathbf{0}_n \\ 1 \\ \mathbf{0}_{n-1} \end{bmatrix}, \quad \mathbf{J} = \begin{bmatrix} \mathbf{0}_{n,n} & \mathbb{1}_n \\ -\mathbb{1}_n & \mathbf{0}_{n,n} \end{bmatrix}, \quad \mathbf{R} = \begin{bmatrix} \mathbf{0}_{n,n} & \mathbf{0}_{n,n} \\ \mathbf{0}_{n,n} & \text{diag}(\gamma_1, \dots, \gamma_n) \end{bmatrix},$$

$$\mathcal{H}(\mathbf{x}) = \sum_{i=1}^n \frac{1}{2} m \mathbf{x}_{n+i}^2 + \sum_{i=1}^{n-1} \left(\frac{1}{2} k_1 (\mathbf{x}_{i+1} - \mathbf{x}_i)^2 + \frac{1}{4} k_2 (\mathbf{x}_{i+1} - \mathbf{x}_i)^4 \right) + \frac{1}{2} k_1 \mathbf{x}_n^2 + \frac{1}{4} k_2 \mathbf{x}_n^4.$$

We rewrite the Hamiltonian by $\mathcal{H}(\mathbf{x}) = \frac{1}{2} \mathbf{x}^\top \mathbf{Q} \mathbf{x} + p(\mathbf{x})$ where

$$\mathbf{Q} = \begin{bmatrix} \mathbf{Q}_0 & \mathbf{0}_{n,n} \\ \mathbf{0}_{n,n} & \mathbb{1}_n \end{bmatrix}, \quad \mathbf{Q}_0 = \begin{bmatrix} 1 & -1 & 0 & \dots & 0 & 0 \\ -1 & 2 & -1 & & & 0 \\ \vdots & & \ddots & \ddots & & \\ 0 & 0 & \dots & -1 & 2 & -1 \\ 0 & 0 & \dots & 0 & -1 & 2 \end{bmatrix},$$

and $p(\mathbf{x}) = \sum_{k=1}^{n-1} \phi(\mathbf{x}_k - \mathbf{x}_{k+1}) + \phi(\mathbf{x}_n)$ with $\phi(x) = \frac{1}{4} x^4$.

In this work, we introduce a coordinate transformation with a new state variable $\hat{\mathbf{x}}$ as follows

$$\hat{\mathbf{x}} = [\ell_1, \dots, \ell_n, \mathbf{x}_{n+1}, \dots, \mathbf{x}_n]^\top, \quad \ell_i = \mathbf{x}_i - \mathbf{x}_{i+1}, \quad i = 1, \dots, n-1, \quad \ell_n = \mathbf{x}_n.$$

We denote $\tilde{h}(\hat{\mathbf{x}}) = \sum_{k=1}^n \phi(\ell_k)$,⁴ and denote $M \in \mathbb{R}^{n \times n}$ as an upper bi-diagonal matrix, with all of its diagonal entries are 1 while all of its sub-diagonal entries being -1 . Then $\hat{\mathbf{x}}$ is the state variable of the system $\Sigma(\tilde{\mathbf{J}}, \tilde{\mathbf{R}}, \tilde{\mathcal{H}}, \tilde{\mathbf{B}}, \mathbf{u}, \mathbf{y}, \hat{\mathbf{x}}_0)$,

⁴The authors of [22] proposed a gradient-preserving adaptive DEIM, which is different from the structure-preserving DEIM that we use. However, for the nonlinear mass-spring-damper system we consider here, these two DEIM approximations are equivalent.

where

$$\begin{aligned} \tilde{J} &= \begin{bmatrix} M & \mathbf{0}_{n,n} \\ \mathbf{0}_{n,n} & \mathbb{I}_n \end{bmatrix}, J = \begin{bmatrix} M & \mathbf{0}_{n,n} \\ \mathbf{0}_{n,n} & \mathbb{I}_n \end{bmatrix}^\top, & \tilde{R} &= \begin{bmatrix} M & \mathbf{0}_{n,n} \\ \mathbf{0}_{n,n} & \mathbb{I}_n \end{bmatrix} R \begin{bmatrix} M & \mathbf{0}_{n,n} \\ \mathbf{0}_{n,n} & \mathbb{I}_n \end{bmatrix}^\top, \\ \tilde{Q} &= \begin{bmatrix} M & \mathbf{0}_{n,n} \\ \mathbf{0}_{n,n} & \mathbb{I}_n \end{bmatrix}^{-\top} Q \begin{bmatrix} M & \mathbf{0}_{n,n} \\ \mathbf{0}_{n,n} & \mathbb{I}_n \end{bmatrix}^{-1}, & \tilde{B} &= \begin{bmatrix} M & \mathbf{0}_{n,n} \\ \mathbf{0}_{n,n} & \mathbb{I}_n \end{bmatrix} B, \\ \tilde{\mathcal{H}}: \hat{x} &\mapsto \frac{1}{2} \hat{x}^\top \tilde{Q} \hat{x} + \tilde{p}(\hat{x}), & \hat{x}_0 &= \begin{bmatrix} M & \mathbf{0}_{n,n} \\ \mathbf{0}_{n,n} & \mathbb{I}_n \end{bmatrix} x_0. \end{aligned}$$

In this example, we investigate this nonlinear mass-spring-damper system where $n = 500$ (i.e., the system dimension is $N = 1000$) on the time interval $(0, 100s]$, with zero initial condition, i.e., $x_0 = \mathbf{0}$. The remaining parameters of the system are set to $k_1 = k_2 = 1$, m_j and $\gamma_j = 0.3$ for $j = 1, \dots, n$. We use a uniform time discretization given by $\Delta t = 10^{-1}s$, resulting in $n_t = 1001$ and two different inputs $u(t) = 0.1$ and $u(t) = 0.1 \sin(t)$ are tested. For the ROMs, we test the GMG-POD-ROM, GMG-QM-ROM and SP2-POD-ROM with the reduced order r from 6 to 20 and we set $\epsilon_{\text{DEIM}} = 10^{-8}$. The tolerance and maximum number of iterations of Newton's method is set to 10^{-8} and 20 respectively. The regularization parameter for the GMG-QM-ROM with reduced-order r is set to $\lambda_{\text{reg}} = \max(0.2 * e_{\text{proj}}(r), 10^{-2.5})$.

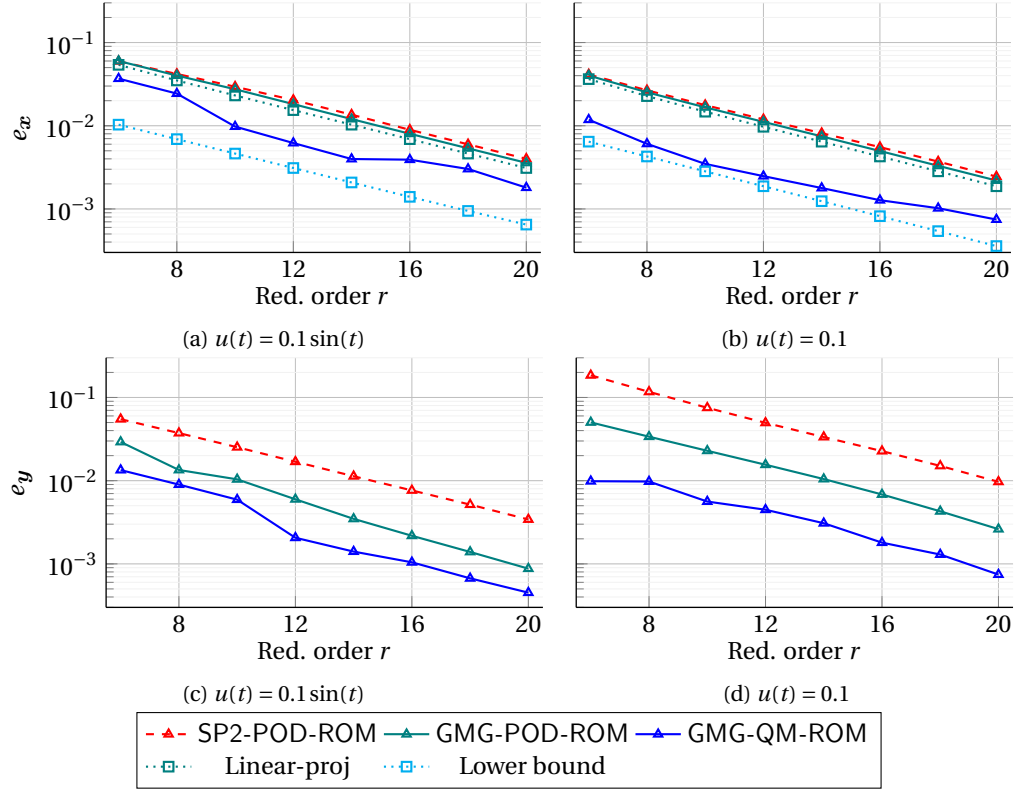


Figure 3: Reduction and output error obtained by SP2-POD-ROM, GMG-POD-ROM, and GMG-QM-ROM for the nonlinear mass-spring-damper system with the inputs $u(t) = 0.1$ and $u(t) = 0.1 \sin(t)$. Linear-app represents the projection error of corresponding linear embedding maps. The lower bound for the ROMs resulting from the quadratic embeddings maps is computed by (28).

Figure 3 shows that the SP2-POD-ROM and GMG-POD-ROM have close performance in terms of the state error, while the GMG-POD-ROM outperforms the SP2-POD-ROM with respect to the output error. By considering a quadratic embedding and the resulting GMG-QM-ROM, both, the state error and the output error, are improved. As for the error in the energy balance equation (3), Figure 4 shows that all these ROMs have a similar error compared to the FOM.

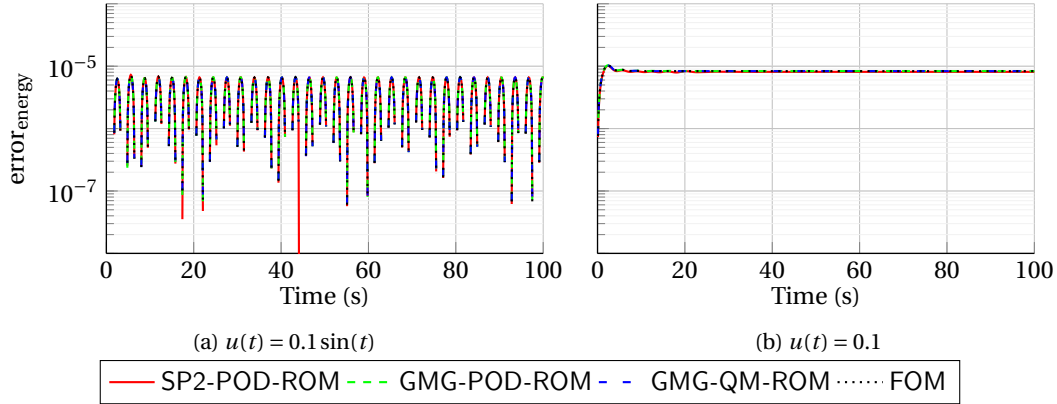


Figure 4: Error in the energy balance equation (30) of the FOM and ROMs with a reduced order of 16 obtained by the SP2-POD-ROM, GMG-POD-ROM, and GMG-QM-ROM for the nonlinear mass-spring-damper system with two different inputs.

6 Conclusion and outlook

We propose a new structure-preserving MOR framework for pH systems with general nonlinear approximation maps based on the GMG projection. We provide two concrete realizations with a linear and a quadratic embedding map for linear and nonlinear pH systems. Numerical examples of a linear and a nonlinear mass-spring-damper system are investigated, and the GMG-POD-ROM and the GMG-QM-ROM provide a lower relative error compared to known methods in the literature in terms of state and output. With respect to future work, we aim to consider different classes of pH systems, e.g., a pH system, where the resistive term is a nonlinear function of $\nabla_x \mathcal{H}(x(t))$ or employing structure-preserving neural networks to speed up the evaluation of a state-dependent systems matrices in a reduced order pH model.

References

- [1] J. Annoni. *Modeling for Wind Farm Control*. PhD thesis, University of Minnesota, 2016.
- [2] A. C. Antoulas, C. A. Beattie, and S. Gugercin. *Interpolatory Model Reduction of Large-Scale Dynamical Systems*, pages 3–58. Springer, 2010. doi:10.1007/978-1-4419-5757-3_1.
- [3] P. Buchfink, S. Glas, and B. Haasdonk. Approximation bounds for model reduction on polynomially mapped manifolds. *Comptes Rendus. Mathématique*, 362:1881–1891, 12 2024. doi:10.5802/crmath.632.
- [4] P. Buchfink, S. Glas, B. Haasdonk, and B. Unger. Model reduction on manifolds: A differential geometric framework. *Physica D: Nonlinear Phenomena*, 468, 2024. doi:10.1016/j.physd.2024.134299.
- [5] F. Califano, R. Rashad, F. P. Schuller, and S. Stramigioli. Geometric and energy-aware decomposition of the Navier-Stokes equations: A port-Hamiltonian approach. *Physics of Fluids*, 33, 4 2021. doi:10.1063/5.0048359.
- [6] S. Chaturantabut, C. A. Beattie, and S. Gugercin. Structure-preserving model reduction for nonlinear port-Hamiltonian systems. *SIAM Journal on Scientific Computing*, 38:B837–B865, 2016. doi:10.1137/15M1055085.
- [7] S. Chaturantabut and D. C. Sorensen. Nonlinear model reduction via discrete empirical interpolation. *SIAM Journal on Scientific Computing*, 32:2737–2764, 2010. doi:10.1137/090766498.
- [8] V. Duindam, A. Macchelli, S. Stramigioli, and H. Bruyninckx. *Modeling and control of complex physical systems the port-Hamiltonian approach*. Springer Science & Business Media, 2009. doi:10.1007/978-3-642-03196-0.
- [9] A. Falaize and T. Hélie. Passive guaranteed simulation of analog audio circuits: A port-Hamiltonian approach. *Applied Sciences (Switzerland)*, 6, 9 2016. doi:10.3390/app6100273.
- [10] Y. Geng, L. Ju, B. Kramer, and Z. Wang. Data-driven reduced-order models for port-Hamiltonian systems with operator inference. *Computer Methods in Applied Mechanics and Engineering*, 442:118042, 7 2025. doi:10.1016/j.cma.2025.118042.

- [11] C. Greif and K. Urban. Decay of the Kolmogorov N-width for wave problems. *Applied Mathematics Letters*, 96:216–222, 2019. doi:10.1016/j.aml.2019.05.013.
- [12] S. Gugercin, R. V. Polyuga, C. Beattie, and A. J. van der Schaft. Structure-preserving tangential interpolation for model reduction of port-Hamiltonian systems. *Automatica*, 48:1963–1974, 2012. doi:10.1016/j.automatica.2012.05.052.
- [13] T. C. Ionescu and A. Astolfi. Families of moment matching based, structure preserving approximations for linear port-Hamiltonian systems. *Automatica*, 49:2424–2434, 2013. doi:10.1016/j.automatica.2013.05.006.
- [14] T. C. Ionescu and A. Astolfi. Moment matching for nonlinear port-Hamiltonian and gradient systems. In *IFAC-Proceedings*, volume 46, pages 395–399, 2013. doi:10.3182/20130904-3-R0-2023.00060.
- [15] B. Jacob and H. Zwart. *Linear Port-Hamiltonian Systems on Infinite-dimensional Spaces*. Springer Science & Business Media, 2012. doi:10.1007/978-3-0348-0399-1.
- [16] Y. Kawano and J. M. Scherpen. Structure preserving truncation of nonlinear port-Hamiltonian systems. *IEEE Transactions on Automatic Control*, 63:4286–4293, 2018. doi:10.1109/TAC.2018.2811787.
- [17] P. Kotyczka and L. Lefevre. Discrete-time port-Hamiltonian systems based on Gauss-Legendre collocation. *IFAC-PapersOnLine*, 51(3):125–130, 2018.
- [18] V. Mehrmann and B. Unger. Control of port-Hamiltonian differential-algebraic systems and applications. *Acta Numerica*, 32:395–515, 2023.
- [19] B. Moore. Principal component analysis in linear systems: Controllability observability and model reduction. *IEEE Transactions on Automatic Control*, 26:17–32, 1981. doi:10.1109/TAC.1981.1102568.
- [20] R. Morandin, J. Nicodemus, and B. Unger. Port-Hamiltonian dynamic mode decomposition. *SIAM Journal on Scientific Computing*, 45:A1690–A1710, 2023. doi:10.1137/22M149329X.
- [21] M. Ohlberger and S. Rave. Reduced basis methods: Success, limitations and future challenges. In *Proceedings of ALGORITHM*, pages 1–12, 2016.
- [22] C. Pagliantini and F. Vismara. Gradient-preserving hyper-reduction of nonlinear dynamical systems via discrete empirical interpolation. *SIAM Journal on Scientific Computing*, 45:A2725–A2754, 10 2023. doi:10.1137/22M1503890.
- [23] R. V. Polyuga and A. J. van der Schaft. Effort- and flow-constraint reduction methods for structure preserving model reduction of port-Hamiltonian systems. *Systems and Control Letters*, 61:412–421, 2012. doi:10.1016/j.sysconle.2011.12.008.
- [24] R. Rashad, F. Califano, A. J. van der Schaft, and S. Stramigioli. Twenty years of distributed port-Hamiltonian systems: A literature review, 12 2020. doi:10.1093/imamci/dnaa018.
- [25] J. Rettberg, J. Kneifl, J. Herb, P. Buchfink, J. Fehr, and B. Haasdonk. Data-driven identification of latent port-Hamiltonian systems. *arXiv preprint arXiv:2408.08185*, 8 2024.
- [26] K. Sato. Riemannian optimal model reduction of linear port-Hamiltonian systems. *Automatica*, 93:428–434, 7 2018. doi:10.1016/j.automatica.2018.03.051.
- [27] P. Schulze. Structure-preserving model reduction for port-Hamiltonian systems based on separable nonlinear approximation ansatzes. *Frontiers in Applied Mathematics and Statistics*, 9:1160250, 2023. doi:10.3389/fams.2023.1160250.
- [28] P. Schwerdtner and M. Voigt. SOB MOR: Structured optimization-based model order reduction. *SIAM Journal on Scientific Computing*, 45:A502–A529, 2023. doi:10.1137/20M1380235.
- [29] L. Sirovich. Turbulence and the dynamics of coherent structures. ii. Symmetries and transformations. *Quarterly of Applied mathematics*, 45:573–582, 1987. doi:10.1090/qam/910463.
- [30] A. J. van der Schaft and D. Jeltsema. Port-Hamiltonian systems theory: An introductory overview. *Foundations and Trends in Systems and Control*, 1:173–378, 2014. doi:10.1561/2600000002.
- [31] T. Wolf, B. Lohmann, R. Eid, and P. Kotyczka. Passivity and structure preserving order reduction of linear port-Hamiltonian systems using Krylov subspaces. *European Journal of Control*, 16:401–406, 2010. doi:10.3166/ejc.16.401-406.